Exploring Rny1-Dependent Clearance of MS2 and HSP30 RNA Decay Fragments in *Saccharomyces cerevisiae*

Hayden K. Low
Molecular Biology
Dr. Jennifer Garcia

Primary Reader: 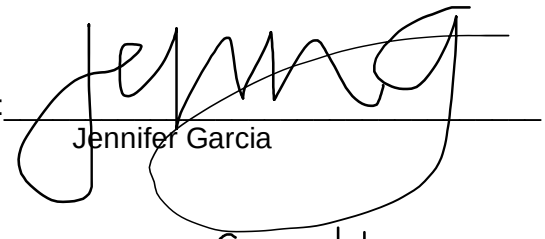
Jennifer Garcia

Secondary Reader: 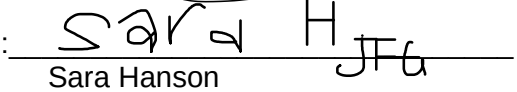
Sara Hanson

Abstract

Tight control over the amount of mRNA through formative and degradative mechanisms is important in regulating many essential cellular processes. Although much focus has been placed on transcriptional regulation, post-transcriptional forms of control such as RNA decay are receiving increasing attention. Recently, evidence suggests that in *Saccharomyces cerevisiae*, certain mRNAs are degraded by a novel route of decay involving autophagic targeting to the vacuole. During the post-diauxic phase, a stage of yeast growth associated with a shift from fermentation to respiration and extensive metabolic changes, apparent alterations in RNA decay and autophagy rates are observed. Specifically, some cytoplasmic RNAs may be subject to targeted autophagic transport to the vacuole, where they may undergo decay by the sole vacuolar ribonuclease Rny1. Our research examines if Rny1 clears persistent molecules called RNA decay fragments that are produced by incomplete cytoplasmic degradation of full-length mRNAs. These persistent decay fragments appear to resist other forms of RNA degradation, such as that mediated by Xrn1, suggesting a previously under-appreciated alternative route of clearance. Using an optimized northern blot procedure, the steady-state levels of these RNA species were monitored in yeast strains with and without Xrn1 or Rny1 activity. Results suggest that active Rny1 is required to effectively clear decay fragments produced from the MS2 array, a well-characterized sequence that can resist cytoplasmic decay. Xrn1 dependence for the formation of MS2 decay fragments was also observed, supporting the hypothesized route of decay fragment production. Similar conclusions were found for decay fragments originating from endogenous transcripts, such as those produced from the heat shock protein 30 (*hsp30*) gene. In both cases, the lack of Rny1 activity appears to cause the accumulation of decay fragments, suggesting that Rny1 is involved in the degradation of persistent byproducts of incomplete cytoplasmic RNA decay. The apparent Rny1-dependent clearance of these MS2 and genomic RNA decay fragments encourages the investigation of additional types of RNA and the elucidation of potential connections to gene regulation and pathology in other eukaryotes.

Examining alternative routes of RNA decay that rely on the highly conserved process of autophagy could ultimately allow for an understanding of dysregulated RNA dynamics and neurodegenerative conditions in mammals.

Introduction

RNA decay as a form of post-transcriptional regulation

Tight regulation over the quantity and localization of mRNA is integral in the control of many essential cellular processes. Although much focus has been placed on the role of transcriptional control in gene regulation, the unique rate at which certain transcripts are produced is only one of the factors determining the extent to which a gene is expressed. A series of post-transcriptional events can occur to control the quantity and translation of RNAs, including localization, sequestration, and degradation. Of these, RNA decay is an especially important point of control for the cell.[i]

Traditionally, studies on RNA decay have focused on cytosolic and nuclear forms of degradation, such as deadenylation, decapping, and destruction via enzymes like Xrn1.[i] Xrn1 is a cytosolic decay enzyme that performs 5' to 3' exoribonuclease activity on uncapped and deadenylated mRNA transcripts. It is responsible for one of the primary routes by which transcripts are removed from the RNA pool and made unavailable for translation. While Xrn1-mediated and other routes of decay are extremely important means of regulating many transcripts, there may be certain RNA species that are not cleared by these methods.[ii] Recently, a novel mechanism of RNA decay has been proposed that relies on the cellular discard and recycling pathway called autophagy.[iii,iv]

Autophagy-mediated RNA decay

Autophagy is the process by which regions of the cytoplasm are enveloped in a double-membrane structure called an autophagosome and trafficked to the lysosome, where the contents are targeted for degradation.[v] Autophagy is a method of removing material such as

defective orangelles, protiens, and macromolecular aggregates from the cytoplasm for degradation in acidified organelles like the lysosome or the vacuole. In *Saccharomyces cerevisiae*, the contents of the autophagosome are deposited in the vacuole.[v] While the role of autophagy in the clearance of cellular proteins and organelles is fairly well-characterized, autophagy-mediated RNA decay remains a relatively understudied area.

Based on our current understanding in yeast, a double-membraned autophagosome forms around cytosolic macromolecules, including RNA, before being transported to the vacuole. The outer autophagosomal membrane fuses with the vacuolar membrane, releasing the inner membrane and enclosed contents into the vacuolar lumen. Once the inner membrane is cleaved, the autophagosomal contents are released and degraded in the acidified environment using a variety of hydrolyases and peptidases. It is predicted that the process of autophagy-mediated RNA decay relies on the action of a degradative enzyme, such as a vacuolar ribonuclease, to degrade RNA.[iv]

After transport by autophagy, the enclosed RNA is subject to some form of vacuolar decay. The sole vacuolar endoribonuclease in *S. cerevisiae*, Rny1, is a primary candidate for the responsible agent.[iii,iv,vi] Rny1 is a member of the T2 RNase family, a type of RNase present in all known organismal classes.[vi] Abnormal T2-family endoribonuclease activity has been implicated in the impaired clearance of rRNAs, the accumulation of amyloid precursor proteins, and white matter lesions in higher eukaryotes, suggesting an important role in maintaining RNA dynamics.[vii] Rny1 degrades RNAs to individual ribonucleotides possessing a 3' phosphate.[iii] In *S. cerevisiae*, Rny1 has already been associated with clearance of rRNAs during ribophagy. Loss of Rny1 resulted in a decrease in decay products produced from rRNA, demonstrating that this ribonuclease is associated with the clearance of RNA in yeast, with a putative role in the processing of ribosomal RNAs during autophagy.**Error! Bookmark not defined.** However, the identities or features of other transcripts subject to this type of decay were still unclear.

RNA decay fragments and the MS2 array

One class of RNA that may be subject to autophagy-mediated RNA decay is RNA decay fragments. RNA decay fragments are smaller pieces of full-length transcripts that are produced by incomplete cytoplasmic degradation. Incomplete cytoplasmic degradation occurs when the action of cytoplasmic decay enzymes such as Xrn1 becomes impeded in some way during RNA decay, resulting in the production of undegraded, stable by-products. While the exact mechanism is not clear, the cytoplasmic decay enzymes may be impeded by the presence of stable secondary structure in the RNA.[viii] It is predicted that specific transcripts, possessing this or other features, may be more likely to produce RNA decay fragments through imcomplete cytoplasmic degradation. For example, previous research suggests that transcripts containing a structure called an MS2 stem-loop array may form RNA decay fragments.

The MS2 array consists of a repeated, virally-derived stem-loop sequence.**Error! Bookmark not defined.** The stem-loop RNA structures are often inserted downstream of the stop codon of a transcript to allow for monitoring and *in vivo* localization of the tagged RNA in live cells. The stem loops are bound and stabilized by MS2 coat protein (MCP) fused to green fluorescent protein (GFP) or another tag.[ii] The fluorescently labelled coat protein is expressed alongside the MS2-containing construct, such that the location of the bound array can be determined using fluorescence microscopy. In addition to allowing localization, it appears that MCP binding to the MS2 stem loops is also able to resist the 5' to 3' progression of Xrn1, inhibiting cytoplasmic decay of the MS2 array and any downstream sequences.**Error! Bookmark not defined.** This inhibition results in the formation of RNA decay fragments from MS2-tagged transcripts.[ii] For the MS2 array, decay fragment formation depends on the presence and binding of MCP to the stem loops as well as the presence of Xrn1.[ii] However, the mechanism by which these decay fragments are cleared from the cell is not accounted for by this process. We predicted that some transcripts showing incomplete cytoplasmic degradation, such as decay fragments originated from the MS2 array, may be subject to an autophagy-mediated form of clearance. If this was the

case, we predicted that the sole vacuolar ribonuclease Rny1 would play an integral role in the elimination of decay fragments from the yeast cell.

RNA decay fragments are targets of Rny1-mediated decay

To determine if Rny1 is involved in the clearance of RNA decay fragments, we examined the steady state levels of decay fragments in yeast strains with and without catalytically active Rny1. According to our predicted mechanism of decay fragment clearance (Figure 1), we would expect that the absence of catalytically-active Rny1 would result in the accumulation of RNA decay fragments. If Rny1-dependent clearance of persistent RNA decay fragments is supported, there would be broad implications, including support for autophagy-mediated RNA decay, a deeper understanding of RNA dynamics in eukaryotes, and a clearer conceptualization of how this process is involved in homeostatic and pathological conditions in mammalian cells.

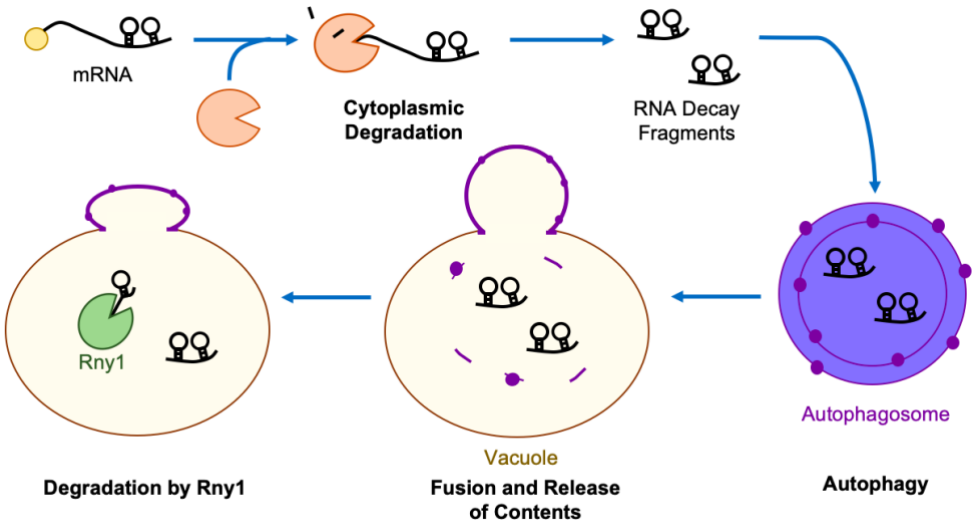

Figure 1: Potential mechanism of Rny1-dependent degradation of RNA decay fragments. mRNAs that experience impaired cytoplasmic degradation produce RNA decay fragments. These decay fragments may be engulfed in autophagosomes. In *S. cerevisiae*, these autophagosomes then release their contents in the vacuole, where the inner-membrane is then lysed. The vacuolar endoribonuclease Rny1 is predicted to be involved in the degradation of these decay fragments.

The biological context of the yeast cell does matter significantly when examining the relevance of a putative autophagy-mediated RNA decay pathway involving Rny1. This is

because autophagy, and thus the transport of cytoplasmic transcripts by this pathway, shows different activity during different phases of yeast growth.[Error! Bookmark not defined.] Due to this, we examined yeast cells during the post-diauxic stage of their growth. This phase occurs after the diauxic shift, when yeast switch from fermentation to respiration and begin using ethanol as a fuel source as glucose becomes depleted.[Error! Bookmark not defined.] During this phase, there are also apparent changes in RNA dynamics, as the cytoplasmic RNA decay enzyme Xrn1 becomes sequestered away from other cytoplasmic decay machinery in eisosomes and shows decreased activity.[ix] This may cause alternative routes of RNA decay, such as the Rny1-dependent mechanism that is hypothesized, to become more important during this time.

Our research seeks to determine if Rny1 is involved in the degradation of RNA decay fragments during the post-diauxic phase. This was done through the monitoring of steady-state levels of full-length and decay fragment molecules using an optimized northern blot procedure. We investigated both exogenous decay fragments produced from transcripts containing an MS2 array, as well as putative decay fragments originating from the yeast gene HSP30. Specifically, we attempted to see if impaired Rny1 activity would result in the accumulation of RNA decay fragments from both of these sources, supporting vacuolar clearance for RNA decay fragments and coinciding with our model for autophagy-mediated RNA decay. By doing so, we hoped to determine if alternative forms of RNA decay involving vacoluar degradation play a significant role in the clearance of some macromolecules during certain phases of yeast growth.

Materials and Methods

RNA Isolation.

Starter cultures were prepared in YPAD or the appropriate SC dropout media and incubated in the rotary incubator at 40% speed and 30°C for 1-3 days. The optical density (OD) of the starter cultures was determined. Cultures were back diluted to an OD = 0.2 in 25 mL in the appropriate media were created. After 20 hrs of growth at 30°C and 200 rpm, an OD of 4-5 was verified. Samples were pelleted at 3000 x g for 5 min and frozen down in liquid nitrogen. The pellets

were stored at -80°C or immediately thawed for 20 minutes followed by resuspension in 500 uL LET. The cells were pelleted at 3000 x g for 30 s and the supernatant was removed. 150 uL LET, ~300 uL of Zirconia beads, and 150 uL of phenol equilibrated with LET (PL) were added and the mixture was vortexed in a multimixer for 5 minutes at top speed. After briefly spinning down, 250 uL of RNase free water and 250 uL of phenol/chloroform equilibrated with LET (PCL) were added. The mixture was vortexed for 30 s and spun at max speed for 5 minutes. The upper aqueous phase was transferred to 400 uL of PCL, vortexed for 30 s, and spun at max speed for 5 minutes. The aqueous phase was separated and 400 uL of chloroform was added. The mixture was vortexed for 20 s and spun down at max speed for 5 minutes. The aqueous phase was added to 40 uL of 3M NaOAC. 400 uL of 100% EtOH was added and the entire mixture was inverted 5-6 times. After a 1 hr incubation at -20°C, the mixture was centrifuged for 10 minutes at max speed and 4 °C. The supernatant was removed and the RNA pellet was washed with 70% EtOH for 5 minutes at max spin speed and room temperature. The supernatant was removed and the RNA pellet was dried in the SpeedVac at room temperature for 15 minutes. The pellet was resuspended in DEPC H2O and analyzed using the Nanodrop and TapeStation machines.

Gel Loading Buffer (1.5X) Preparation.

Ultrapure formamide to a final concentration of 95%, 2.5% bromophenol blue to a final concentration of 0.025%, 2.5% xylene cyanol FF to a final concentration of 0.025%, and 0.5 M, pH 8.0 EDTA to a final concentration of 5 mM were combined to create 1.5X RNA Gel Loading Buffer.

AlexaFluor Dye Conjugation to Amino Labeled Probe.

4.17 ug of amino-labeled probe was incubated at 65°C for 5 minutes. The probe was placed on ice for 3 minutes then centrifuged at 10000 x g for 3 minutes. An 84 mg/mL solution of sodium bicarbonate was created and 3 uL of the solution was added to the probe. The AlexaFluor dye was resuspended in 2 uL of DMSO and vortexed at high speed for 10 s. 2 uL of the dye was

added to the probe mixture. The mixture was vortexed at maximum speed for 30 s and spun down briefly. The labeling reaction was incubated at room temperature for 1 hour in the dark. The dye was diluted 10-fold. DNA cleanup binding buffer was added to the labeling reaction along with 100% ethanol prior to mixing. The labeling reaction, DNA binding buffer, and ethanol mixture was transferred to a Monarch kit column and spun at 16000 x g for 1 minute. DNA wash buffer with added ethanol was deposited on the column. The column was spun at 16000 x g for 1 minute. MB water was added to the column and the probe was eluted after waiting 4 minutes by spinning at 16000 x g for 1 minute. The success of the labeling reaction was determined using the Nanodrop machine on the microarray setting.

Agarose + Formaldehyde Gel Electrophoresis.

RNA samples were thawed on ice for 30 minutes. 10X DEPC-treated MOPS (52.25 mg/mL of MOPS pH = 7.0 using NaOH) was diluted to 1X. A 1.25% agarose gel was created with 1X MOPS, 1X GelRed, and 0.7% formaldehyde. The Kerafast biotinylated sRNA ladder was prepared using a 1/20 dilution in 1.5X Gel Loading Buffer. 10 ug RNA samples were prepared in Gel Loading Buffer to a final concentration of 1-1.5X. The SpeedVac was used to pellet the RNA if required. The DynaMarker RNA High Ladder was prepared with 1 ug of ladder and a 3:5 dilution of the included RNA loading buffer. All ladders and samples were heated to 65°C for 3 minutes and placed on ice prior to loading. The gel was primed with 1X MOPS and run at 70V for 3.5 hrs. The gel was imaged using the iBright FL1000.

Capillary Transfer.

A container with 10 gel volumes of 10X SSC (diluted from 20X SSC: 219.13 mg/mL NaCl and 110.25 mg/mL sodium citrate, HCl pH = 7.0) was prepared. Two wicking filter papers and think blotting paper were placed on a solid foam support. The gel was flipped upside down and placed on the bottom supports. A nitrocellulose membrane, two layers of filter paper, and absorbent cloth material were placed on the gel followed by compression with a glass plate and

two circle weights. The RNA was allowed to transfer for 16-24 hours. The membrane was cross-linked and the gel was imaged using the iBright FL1000 to analyze the success of the transfer.

Hybridization and Detection Using Chemiluminescence.

The membrane was pre-hybridized in Denhardt's hybridization buffer (6X SSC, 10X Denhardt's, 0.1% SDS) for 3 hrs at 42°C. 10 pmol of biotinylated probe was added to the hybridization buffer after decanting from the hybridization tube. The probe-buffer mixture was briefly mixed and returned to the hybridization tube. The membrane was hybridized overnight at 42°C. The membrane was washed twice at room temperature for 5 minutes and once at 37°C for 20 minutes in 6X SSC + 0.1% SDS. Four wash steps were completed for 5 minutes each at room temperature in 1X SSC + 0.1% SDS. Substrate equilibration buffer was added to the membrane for 5 minutes with shaking at room temperature. Equal parts stable peroxide solution and luminol solution were combined and mixed. The membrane was blotted dry on a paper towel and the peroxide-luminol solution was used to coat the membrane. After 5 minutes, the membrane was imaged on the iBright FL1000. To reprobe the membrane, it was first stripped by microwaving in 0.1X SSC + 0.1% SDS for 10 minutes.

Hybridization and Detection Using Fluorescence.

The membrane was pre-hybridized in Denhardt's hybridization buffer for 3 hrs at 42°C. 10 pmol of radiolabeled probe was added to the hybridization buffer after decanting from the hybridization tube. The probe-buffer mixture was briefly mixed and returned to the hybridization tube and the membrane was hybridized overnight at 42°C. The membrane was washed at room temperature for 10 minutes once in 2X SSC + 0.1% SSC and once in 1X SSC + 0.1% SSC. The membrane was imaged using the fluorescent blot setting and the appropriate dye filters with the iBright FL1000.

Image Analysis and Signal Quantification.

Membranes were imaged with the saturation setting turned off. Contrast and exposure were adjusted in ImageJ. The ImageJ measure function was applied to the inverted membrane image to determine the integrated density of each band.

Miniprep Isolation of pRny1.

A bacterial culture was made in LB-Carb liquid media and grown at 37°C overnight. Cells were pelleted at 5000 x g for 30 s and the supernatant was removed. The pellet was resuspended in A1 buffer. A2 buffer was added and the solution was inverted until it was completely mixed. A3 buffer was added and inverted until there was no blue coloration visible. The solution was spun at 13000 x g for 5 minutes. The supernatant was transferred onto an MN column placed on a vacuum manifold. The supernatant was passed through the column using a vacuum pump and PE buffer was added to the column. The PE buffer was passed through the column using the vacuum pump and the column was spun dry at 13000 x g for 2 minutes in a collection tube. MB water was added to the center of the column and allowed to sit for 4 minutes at room temperature. The liquid was captured by spinning at 7000 x g for 1 minute. The isolated DNA was quantified using the Nanodrop.

Yeast Transformation Using LiOAc/TE and PEG/LiOAc.

Cultures were prepared in YPAD or the appropriate SC knockout media and incubated in the rotary incubator at 40% speed and 30°C overnight. The OD of the overnight cultures was determined and OD 0.2 back-dilutions to 5 mL of the appropriate media were created. After 5 hrs of growth at 30°C and 200 rpm, the cells were pelleted at 2000 rpm for 5 minutes. The supernatant was removed and the pellet was resuspended in 1 mL of LiOAc/TE (100 mM pH 7.5 LiOAc, 10 mM pH 8.0 Tris/HCl, 1 mM pH 8.0 EDTA). The cells were pelleted at 2000 rpm for 5 minutes, the supernatant was removed, and the pellet was resuspended in 100 uL of LiOAc/TE. 2 ug of plasmid DNA was added along with 10 uL of 10 mg/mL ssDNA boiled at 100°C for 5 minutes and chilled on ice. The mixture was vortexed and incubated at 30°C for 15 minutes. 500 uL of PEG/LiOAc (40% PEG, 100 mM pH 7.5 LiOAc, 10 mM pH 8.0 Tris/HCl, 1

mM pH 8.0 EDTA) was added and the mixture was vortexed. The cells were kept in a 42°C water bath for 10 minutes and pelleted at 2000 rpm for 3 minutes. The supernatant was removed and the pellet was resuspended in 100 uL of YPAD or the appropriate SC knockout media. The cells were plated on the appropriate YPAD or SC knockout plate. Plates were grown at 30°C for 1-2 days.

SC Media Preparation.

Reagents were added to a final concentration of 1X YNB, 1.47 mg/mL of -Ade-His-Leu-Lys-Met-Ura Dropout Mix, 2% glucose and the appropriate 1X Ade, 1X Lys, 1X Met, and 1X Leu stocks, considering the necessary dropouts. The mixture was pH balanced to 6.0 using 6M NaOH and autoclaved on the liquid media setting.

SC Plate Preparation.

Reagents were added to achieve a final concentration of 1.70 mg/mL of YNB, 5.00 mg/mL ammonium sulfate, and 20.00 mg/mL Bactoagar and stirred until hydrated. The mixture was microwaved for 2 minutes and autoclaved on the liquid media cycle. The mixture was cooled while stirring and reagents were added to a final concentration of 2% glucose, 1.47 mg/mL of -Ade-His-Leu-Lys-Met-Ura Dropout Mix, and the appropriate 1X Ade, 1X Lys, 1X Met, and 1X Leu stocks considering the necessary dropouts.

Results

Exogenous, MS2-containing and endogenous transcripts produce putative decay fragments

To examine the role of Rny1 in the clearance of RNA decay fragments, we investigated two different transcripts that demonstrated the potential for decay fragment formation. The first was an exogenous, MS2 array-containing construct expressed in conjunction with MCP. The specific construct we were investigating was a fusion of the *PGK1* coding sequence and a 3' set of 24 MS2 stem-loops in an array. The 24xMS2 array was inserted downstream of the coding sequence and a doxycycline-repressible promoter. Figure 2 shows the predicted mechanism by which *PGK1-24xMS2* undergoes incomplete cytoplasmic degradation in the presence of MCP, producing RNA decay fragments that consist of the MS2 array and any downstream sequences. A central aspect of this model is the Xrn1 dependence for the partial degradation of the full-length transcript. This was previously demonstrated in data collected by Dr. Jennifer Garcia, in which *xrn1*Δ yeast showed more full-length MS2-containing transcripts and highly impaired decay fragment formation. Although this previous work verifies that Xrn1 is involved in the formation of MS2 decay fragments, our work investigates the agents responsible for the clearance of the persistent RNA decay fragments that are produced.

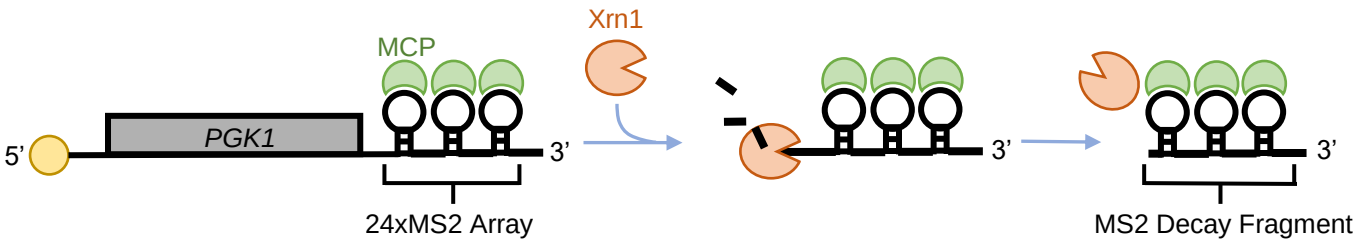

Figure 2: MS2 decay fragments are produced by impaired cytoplasmic degradation of *PGK1-24xMS2* transcripts. An array of 24 MS2 stem loops was inserted downstream of the coding sequence for *PGK1*. The transcript undergoes 5' to 3' degradation via Xrn1 after deadenylation and decapping. This degradation is impeded by the highly structured MS2 array when the stem loops are bound by MS2 coat protein (MCP), resulting in the production of highly-structured MS2 decay fragments.

Although MS2-containing RNA allows for the reproducible and controlled production of RNA decay fragments, RNA-seq data performed by Garcia *et al.* suggests that endogenous transcripts may undergo a similar process. The endogenous transcript of interest was the mRNA produced from the heat shock protein 30 (*hsp30*) gene. HSP30 is a protein involved in the coordinated stress response against the effects of heat on the plasma membrane of *S. cerevisiae*.[x] A relative abundance of RNA-seq reads in two regions suggests the production of two RNA decay fragments from this transcript (Figure 3). Similar to the decay fragments produced from the MS2 array, those produced from *HSP30* may be formed by incomplete cytoplasmic decay and targeted to the vacuole by autophagy. Understanding any potential non-cytosolic routes of RNA decay for endogenous transcripts would be of utmost importance in developing a more complete picture of how the amount of RNA, especially that of persistent RNA molecules prone to accumulation, is regulated in *S. cerevisiae*.

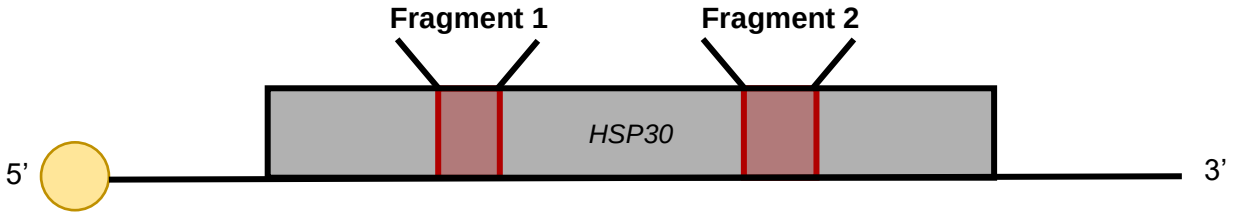

Figure 3: Endogenous *HSP30* transcripts produce two RNA decay fragments. Reads from two regions of the *HSP30* transcript appear to be overrepresented in the RNA-seq data, suggesting that these sequences form stable fragments.

Optimized northern blot procedure allows for specific detection of RNA species.

To probe the agents and pathways involved in the formation and clearance of RNA decay fragments, we required a method for detecting these species. Chemiluminescent northern blot was used as a method of detecting and quantifying full-length RNA and decay fragments and quantifying them under various conditions. This method uses a specific oligonucleotide probe with an attached biotin hapten, which allows for binding to streptavidin-

horse radish peroxidase (HRP) and secondary detection of a chemiluminescent reaction. To separatate RNA for detection using northern blot we used a denaturing agarose + formaldehyde gel. Optimal separation of the prominent *25S* rRNA, *18S* rRNA, and low molecular weight RNA species appeared to occur after 3.5 hours of electrophoresis at 70V (Lane 1, Figure 4A). Distinct bands were observed for the *25S* rRNA band (upper band) and the *18S* rRNA band (lower band). These bands appeared visually prominent due to their relative abundance compared to other RNA species. Their distinct nature and lack of smearing demonstrates minimal degradation of the abundant *18S* and *25S* rRNA species, and by extension, the total RNA isolate as a whole. A lack of degradation was essential over the course of this experiment, as our analysis hinged upon the accurate quantification of RNA species under various cellular conditions. Generalized degradation occurring during or after RNA isolation would confound the quantification of full-length transcripts and decay fragments, which would prevent us from accurately determining the role of Rny1 in decay fragment clearance. Finally, a prominent, diffuse band was located at the bottom of lane 1, which likely corresponds to low molecular weight species such as tRNAs.

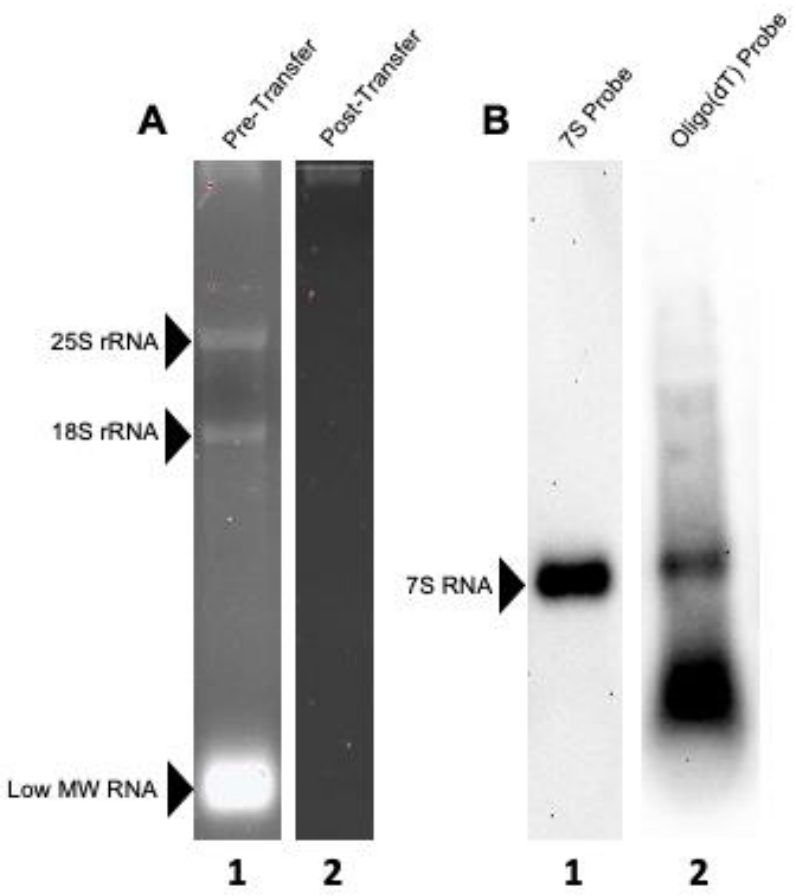

Figure 4: Agarose + formaldehyde gel electrophoresis and capillary transfer allow for the robust detection of *7S* and poly-adenylated RNA. (A) Agarose + formaldehyde gel electrophoresis provides sufficient separation of the *25S* rRNA, the *18S* rRNA, and low molecular weight (MW) RNA, which are all highlighted by black arrows. Capillary transfer appears to have been successful at removing RNA from the gel. (B) Treatment with the *7S* probe allows for the detection of *7S* RNA, which is highlighted with a black arrow. Treatment with the oligo(dT) probe allows for the detection of polyadenylated RNA. The presence of a well-defined signal suggests a functional northern blot procedure for these RNA species.

In order to detect specific RNA, the gel was transferred to a nitrocellulose membrane. To test if extensive transfer was successful, a capillary transfer set-up was completed and the membranes were probes against constitutively expressed *7S* and poly-adenylated RNA. Using 10X SSC buffer and an absorbent cloth material, overnight transfer appeared to be highly successful as demonstrated by the lack of RNA material that remained in the gel (Lane 2, Figure 4A). As expected, only a small amount of high molecular weight RNA is visible in the gel due to the increased resistance to transfer encountered by longer molecules. The lack of

material in the gel suggested adequate transfer, but it was the detection of *7S* and polyadenylated RNA using the appropriate probes that demonstrated the success of this method. Using the *7S* probe (Table 1), detection of a prominent band corresponding to the constitutively expressed *7S* RNA was achieved (Lane 1, Figure 4B). The lack of obvious smearing demonstrates minimal RNA degradation as well. The detection of *7S* RNA without significant background means that when using the appropriate probes, the separation, transfer, hybridization, and imaging steps used in the procedure are capable of detecting RNA. Similar results were observed for poly-adenylated RNA detected using an oligo(dT) probe after membrane stripping and reprobing (Table 1). Clear regions of banding were present, with a prominent signal at the bottom of the lane (Lane 2, Figure 4B). Detection of constitutively expressed *7S* RNA and poly-adenylated RNA using the novel northern blot protocol demonstrated a working procedure that only required further optimization for the detection of *MS2*-containing RNA. Overall, separation, transfer and detection seemed to sufficient to dectect full length mRNAs and RNA decay fragments in *rny1* mutants.

PGK1-24xMS2 produces decay fragments detectable by chemiluminescent northern blot.

To detect and quantify the MS2-containing RNA derived from *PGK1-24xMS2*, we utilized a chemiluminescent northern blot and a probe specific to the MS2 array. By quantifying the relative amount of MS2 array present, we hoped to determine the relative abundance of both full-length MS2-containing constructs and MS2 decay fragments, allowing us to visualize whether Rny1 catalytic activity is required for normal clearance of these decay fragments. The probe being used had previously demonstrated success identifying *MS2*-containing RNA using the radioactive northern blot method (Table 1). This sequence binds to a single region near the 3' end of the MS2 array. However, the biotin-marked version of the 3' MS2 probe did not allow for sufficient detection in our chemiluminescent northern blot procedure (data not shown). In order to increase assay sensitivity by adjusting hybridization efficiency and wash stringency, a homemade Denhardt's hybridization buffer was used and wash temperatures, durations, and

buffers were changed. Specifically, the temperature and duration of the wash steps were decreased, and a less stringent 6X SSC + 0.1% SSC buffer was used during the stringency wash steps. Following these changes, there was still inadequate detection of MS2-containing RNA for quantification and analysis (data not shown). Because detection of constitutive *7S* RNA was still occurring with high success, alterations to the probe sequence were deemed most likely to result in successful detection of *MS2*-containing RNA.

In order to detect *MS2*-containing transcripts and RNA decay fragments, the appropriate probes detecting the MS2 array had to be created. Because detection with the original 3' MS2 probe proved to be insufficient, three additional probes were created for potential detection of the MS2 array. These consisted of a 5' probe binding once to the upstream portion of the array, an internal probe binding twelve times to the MS2 stem loop sequences, and an additional 3' probe binding to a unique location on the downstream portion of the array (Table 1). Using the northern blot procedure with all four MS2 probes in combination, were were able to detect a larger MS2-containing RNA species and a smearing of smaller MS2-containing species. As expected, there was no apparent signal from the -MS2 lanes which contained RNA isolated from strains that do not express *PGK1-24xMS2* (Lanes 3, Figure 5A; Lane 3, Figure 5B), suggesting that off-target binding was not a major occurrence. The presence of two distinct bands suggested that detection of both full-length *PGK1-24xMS2* RNA and MS2 decay fragments was achieved (Lane 2, Figure 5A). The upper band is likely from the abundant full-length *PGK1-24xMS2* species. There was light smearing beneath this upper band, likely from intermediate decay products produced by the 5' to 3' exoribonuclease activity of Xrn1. The lower band consists of intact MS2 decay fragments that resist degradation. Light smearing is visible beneath this lower band as well, potentially from the progressive degradation of the MS2 array. Additionally, there was still suboptimal detection of both full-length RNA and decay fragments from the WT strain (lane 1, Figure 5A).

Having shown adequate detection of full-length and decay fragment RNA, we could quantify the abundance of decay fragments to determine if Rny1 is involved in their clearance. The robust detection of decay fragment RNA from the *rny1Δ* strain was highly promising (Lane 2, Figure 5A). If Rny1 is the ribonuclease responsible for the clearance of RNA decay fragments, we should see an accumulation of decay fragments relative to the amount of full-length transcript that is transcribed after *Rny1* is knocked out. In Lane 2, two distinct bands were produced. The apparent relative abundance of MS2 decay fragments in the *rny1Δ* strain relative to WT provides support for the involvement of the vacuolar endoribonuclease Rny1 in the clearance of MS2 decay fragments. However, apparent differences in the amount of full-length *PGK1-24xMS2* being expressed may have confounded these observations. Normalizing to the signal from the full-length *PGK1-24xMS2* RNA (Figure 5B), this apparent abundance is supported. The relative abundance of MS2 decay fragments normalized to the amount of full-length *PGK1-24xMS2* present is 5.80 times greater in the *rny1Δ* strain relative to WT. This provides strong evidence in favor of MS2 fragment accumulation in the absence of Rny1, in a manner that is independent of the amount of full-length *PGK1-24xMS2* that is expressed. By accounting for differential *PGK1-24xMS2* transcription by normalizing to the full-length signal, we can assume that the observed differences in decay fragment accumulation are due to differences in decay fragnment clearance. Because the knockout of *Rny1* appears to impair this process, the involvement of Rny1 in the clearance of MS2 decay fragments via a vacuolar route of decay is plausible.

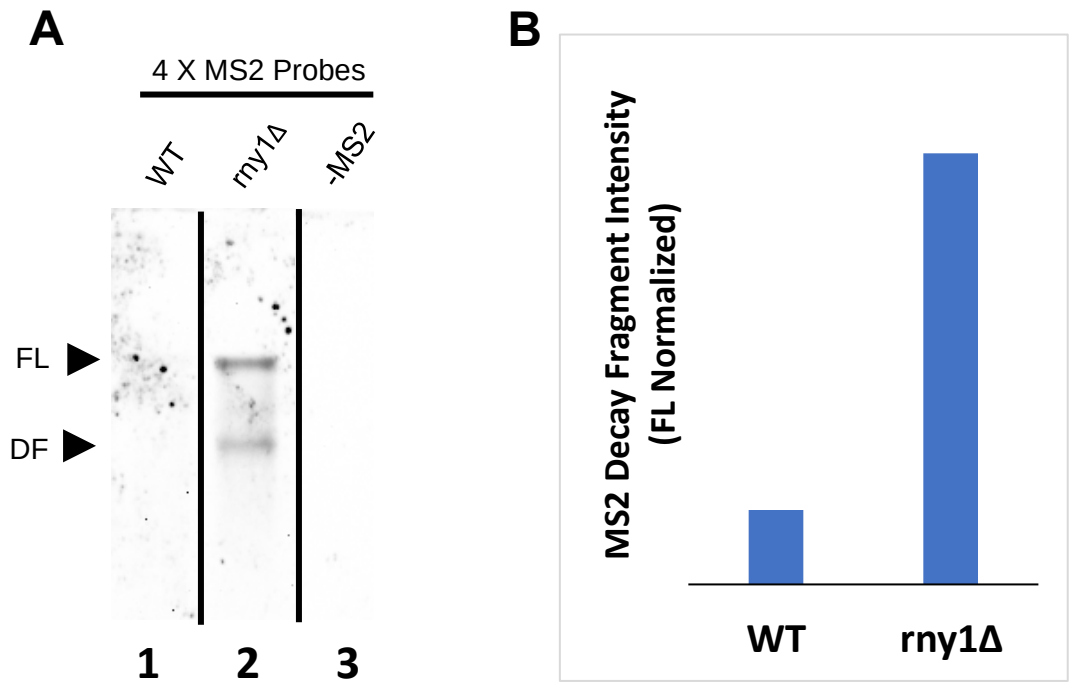

Figure 5: All four MS2 probes combined produce a detectable signal for full-length *PGK1-24xMS2* and MS2 decay fragments. (A) a clear signal is observed for the *rny1Δ* strain when using all four MS2 probes in combination. The upper band (highlighted with a black arrow and labeled FL) likely corresponds to full length *PGK1-24xMS2* (3071 bp). The light smearing beneath the upper band is likely decay intermediates from partial 5' to 3' degradation. A lower band (highlighted with a black arrow and labeled DF) is observed with light smearing beneath it, likely corresponding to the complete MS2 decay fragments (1723 bp) and subsequent decay products. (B) The signal intensity from the full length and decay fragment regions from the membrane in panel A.

MS2 decay fragment formation requires Xrn1.

Having created an efficient method of detecting MS2-containing RNA, verification of the predicted mechanism of MS2 fragment creation could be performed. The cytoplasmic exoribonuclease Xrn1 is one of the primary enzymes involved in the degradation of mRNA in yeast. In order to verify that Xrn1 is involved in decay fragment formation, we compared the relative amounts of MS2 decay fragments in WT and *xrn1Δ* strains. We expected that decay fragments should appear in the WT strain, in which Xrn1 levels were intact, but should be absent upon the knockout of Xrn1. As a negative control, doxycycline was used to repress the expression of *PGK1-24xMS2* from the *tet-off* promoter. This was done to verify that northern blot did not produce any signal in the absence of MS2-containing RNA. As expected there was

an absence of signal in all of the +Dox lanes, suggesting sufficient repression of *PGK1-24xMS2* expression in the presence of doxycycline (Lane 4-6, Figure 6A). There is also no signal observed from the -MS2 yeast strain that does not encode *PGK1-24xMS2* even in the absence of doxycycline (Lane 7, Figure 6A). The minimal detection of MS2-containing RNA from WT yeast was not expected (Lane 1, Figure 6A), and may be due to patterns of *PGK1-24xMS2* expression from the promoter that were not expected. This does not impair our analysis of other lanes however, which still support the Xrn1 dependent formation of decay fragments.

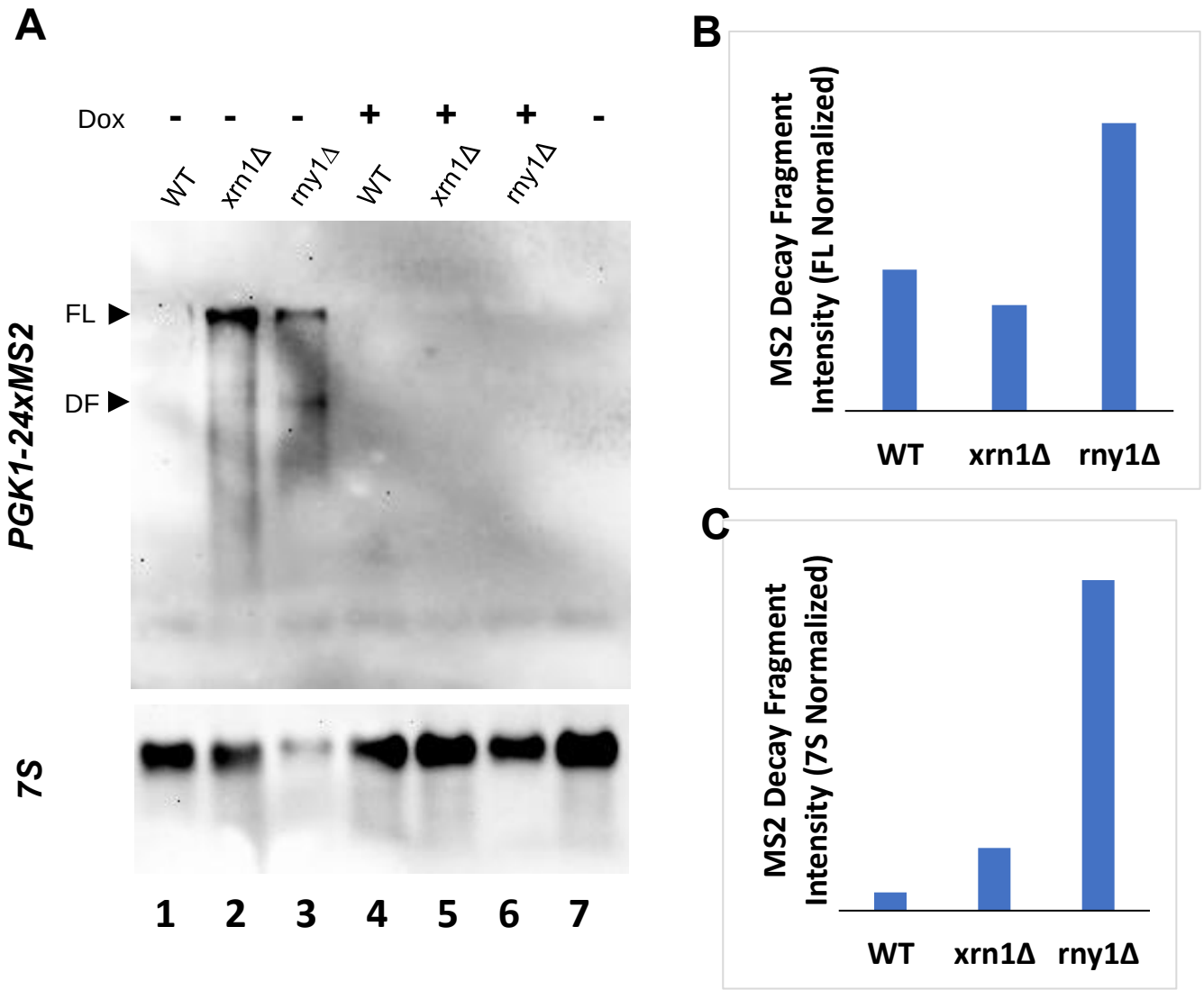

Figure 6: MS2 decay fragment production is XRN1-dependent. Full length *PGK1-24xMS2* is observed for the –Dox samples only. Although we observe full-length *PGK1-24xMS2* (highlighted with a black arrow and labeled FL) in the xrn1Δ sample, no putative decay fragment band is formed. We see a much more prominent decay fragment band in the *rny1Δ* lane (highlighted with a black arrow and labeled DF) as well as a full length *PGK1-24xMS2* band. Below each distinct band is visible smearing, likely from intermediate decay products. A *7S* positive control shows a consistently strong signal with some evidence of degradation for all lanes except the apparently weak signal in the *rny1Δ* – Dox sample.

The Xrn1 dependence of decay fragment formation was supported by the signal pattern observed upon *Xrn1* knockout. The *xrn1Δ* lane shows a very prominent full-length signal and a decay fragment signal that is extremely weak (Lane 2, Figure 6A). Instead of an obvious decay fragment band, there is light smearing across the entire lane that is likely from alternative routes of RNA decay that do not depend on Xrn1 or sample degradation during RNA isolation. The lack of a prominent decay fragment band strongly supports the hypothesized route of decay fragment formation, which involves incomplete cytoplasmic decay via Xrn1 that is inhibited by the MCP-stabilized MS2 array. Additionally, this result strongly suggests that the putative MS2 decay fragment band observed during northern blot was correctly identified. This visual analysis was supported by a numerical quantification of the signal intensities from the full-length and decay fragment regions.

Before we could compare the amount of decay fragments produced in WT and *xrn1*Δ yeast, we had to account for potential differences in detection and full-length transcript production between lanes by normalizing to the full-length signal. By normalizing to the amount of full-length transcript, the relative abundance of decay fragments is based on differences in their route of decay or formation and not influenced by overall differences in *PGK1-24xMS2* expression from the plasmid. After normalization, the signal produced by the MS2 decay fragment region in the -Dox samples produced the expected trends in relative signal intensity. The *xrn1Δ* strains produce slightly fewer decay fragments (0.75X WT expression) due to a lack of cytoplasmic 5’ to 3’ degradation (Figure 6B). The apparent impaired formation of decay fragments is less clear when normalizing to constitutively expressed 7S RNA (relative abundance of MS2 decay fragments is 3.45X WT expression in the *xrn1Δ* strain), potentially due to slight differences in *PGK1-24xMS2* transcription between strains (Figure 6C). Because expression of *PGK1-24xMS2* occurs from the *adh1* promoter, a promoter that is normally involved in the expression of an enzyme essential for ethanol metabolism, differences in growth states between strains at the time of sampling might affect the amount of MS2-containing RNA

that is expressed and confound trends in MS2 decay fragment abundance. To avoid this confounding variable, our analysis focused on the full-length normalization data. In this dataset, the absence of *Xrn1* caused a significant reduction in decay fragment formation. This is in accordance with our model, which suggests that Xrn1 is required for the incomplete degradation of full-length MS2-containing RNA. Overall, the hypothesized Xrn1-dependent pathway of MS2 decay fragment formation is supported during northern blot.

Rny1 is involved in the clearance of MS2 decay fragments.

In order to determine if Rny1 catalytic activity is involved in the clearance of RNA decay fragments, we attempted to observe the accumulation of RNA decay fragments after the removal of Rny1 activity. To rule out any potential confounds from non-catalytic secondary effects of the Rny1 structure, some *rny1Δ* yeast strains were transformed with a plasmid expressing either a catalytically active or inactive form of Rny1. The catalytically inactive version of Rny1 contained two point mutations (H87F, H160F) that prevent RNA cleavage without seriously affecting the structure of Rny1.[Error! Bookmark not defined.] If clearance of RNA decay fragments is dependent on Rny1, we expected to see an accumulation of RNA decay fragments in *rny1Δ* yeast strains. Rescue of the WT phenotype was expected to occur when functional Rny1 was expressed from a plasmid (p*RNY1*) in *rny1Δ* strains, meaning that a reduction in RNA decay fragment levels was anticipated. Because we hypothesized that Rny1-dependent clearance of RNA decay fragments requires the catalytic ribonuclease activity of this enzyme, a similar rescue of the WT phenotype was not expected to occur when catalytically inactive Rny1 was expressed from a plasmid (p*RNY1-ci*) in *rny1Δ* strains.

In order to do so, steady state levels of MS2 decay fragments were compared in WT yeast, *rny1Δ* yeast, and *rny1Δ* yeast with attempted rescue using catalytically active or inactive plasmid-encoded *Rny1*. We expected that catalytically active Rny1 would be required for the clearance of MS2 decay fragments, meaning that a decay fragment band of decreased intensity was anticipated in the WT and *rny1Δ* strain rescued with active Rny1. As predicted, there is no

observed signal in the -MS2 strain incapable of expressing MS2-containing RNA (Lane 5, Figure 7A). In WT, there is clear expression of full-length *PGK1-24xMS2*, however, there appears to be limited steady-state levels of MS2 decay fragments (Lane 1, Figure 7A). In comparison, the relative amount of MS2 decay fragments appears to increase dramatically as *Rny1* is knocked out, suggesting this enzyme's involvement in the clearance of MS2 decay fragments (Lane 2, Figure 7A). Across all lanes, a broader MS2 decay fragment band is observed relative to other blots, potentially due to the usage of 4 different MS2 probes that to bind different sites, causing the formation of multiple decay fragment bands with different sets of bound probes as the target sequence is degraded.

Attempted rescue of the WT phenotype with the addition of catalytically active, plasmid-encoded Rny1 did appear to cause a visual reduction in the amount of MS2 decay fragments (Lane 3, Figure 7A). Although the intensity of the entire lane is lower, attempted rescue with catalytically inactive Rny1 did not appear to decrease the abundance of MS2 decay fragments relative to the amount of full-length transcript that was present compared to the *rny1Δ* strain (Lane 4, Figure 7A). This visual interpretation is supported by the intensity of the MS2 decay fragment bands normalized to the full-length signal. We see a relative abundance of decay fragments in the *rny1Δ* and *rny1Δ* + catalytically inactive Rny1 strains (1.69X and 2.69X WT expression respectively), likely due to impaired clearance (Figure 7B). In comparison, the addition of catalytically active Rny1 appeared to cause near complete rescue of the WT phenotype (1.17X WT expression). The relative abundance of MS2 decay fragments in the *rny1Δ* strain with catalytically inactive Rny1 added appears to disappear when normalizing to the 7S signal, potentially highlighting differences in *PGK1-24xMS2* expression between strains (Figure 7C). Overall, it appears that the catalytic endoribonuclease activity of Rny1 is associated with a lower relative abundance of MS2 decay fragments, suggesting its involvement in their clearance.

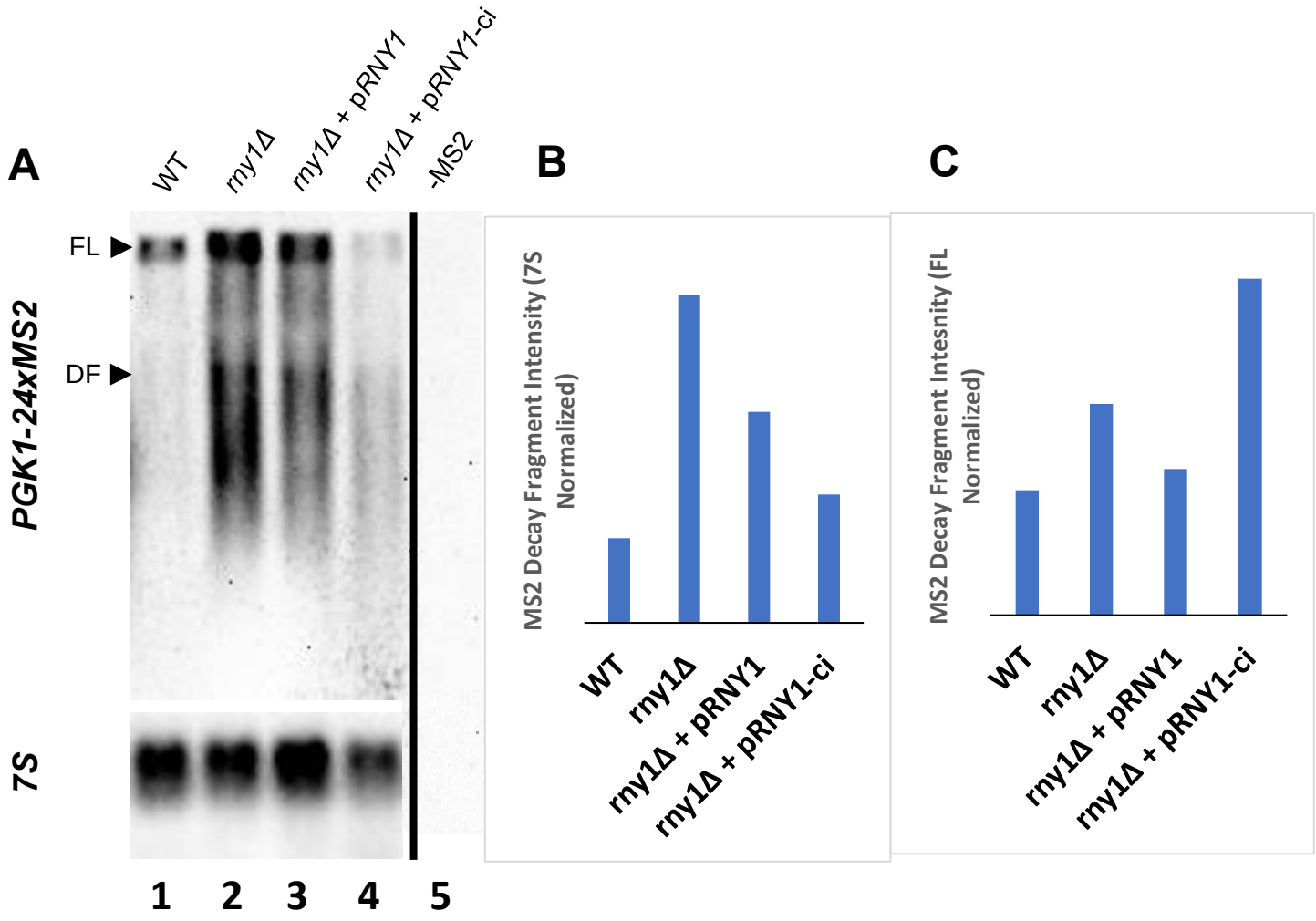

Figure 7: Rny1 activity is involved in the clearance of MS2 decay fragments. Full length *PGK1-24xMS2* (highlighted with a black arrow and labeled FL) is observed for all samples except the –MS2 negative control. The apparent quantity of MS2 decay fragments (highlighted with a black arrow and labeled DF) appears to be increased in the *rny1Δ* strain relative to WT, suggesting an accumulation of decay fragments and potentially impaired clearance. This relative abundance mostly disappears upon the reintroduction of active Rny1 from a plasmid (p*RNY1*). The abundance of the decay fragments relative to the full-length RNA appears to increase if catalytically inactive Rny1 is added from a plasmid (p*RNY1*-ci), suggesting that it is the catalytic activity of Rny1 that is involved in decay fragment clearance.

Rny1 is involved in the clearance of endogenous decay fragments from HSP30.

With supportive evidence for Xrn1-dependent formation and Rny1-dependent clearance of MS2 decay fragments, we could now investigate whether endogenous decay fragments produced by genomic transcripts were also subject to a route of decay involving Rny1 in the post-diauxic phase. Investigating the transcript from the *Hsp30* gene using fluorescent northern blot, we observed robust detection of both full-length *HSP30* and the upstream fragment

targeted by the frag 1 probe. The 3' probe binds a region outside of the two potential fragments, meaning that it should only identify full length *HSP30*. The 3' probe alone allowed detection in all four strains (Lanes 1-4, Figure 8A), with more robust detection for the *rny1Δ* strains (Lanes 2-4, Figure 8A). No decay fragments were identified with the 3' probe as expected. Because the sequence contained in fragment 1 is also present in full-length *HSP30*, the frag 1 probe was able to detect both putative *HSP30* decay fragments as well as full length *HSP30* for all strains (Lanes 1-4). The relative intensity of the decay fragments is higher in the *rny1Δ* and *rny1Δ* with catalytically inactive Rny1 strains (Lanes 2 and 4), as would be expected if Rny1 activity was involved in their clearance. The WT strain appears to have the lowest steady state level of decay fragments (Lane 1), while *rny1Δ* with catalytically active Rny1 added has a steady-state level that is still much lower compared to the other *rny1Δ* strains (Lane 3). The composite image shows these relative trends for full-length and decay fragment abundance for *HSP30* across the four strains. The relative intensity of the *HSP30* decay fragment signal is supported in the full-length normalized data (Figure 8B). Due to a lack of 7S data, only full-length normalization was performed. This normalization incorporates any potential differences in *HSP30* expression between strains. Knocking out *Rny1* causes a slight increase in the abundance of putative *HSP30* decay fragments (1.25X WT expression), an increase that is largely reversed by reintroduction of Rny1 expression from a plasmid (1.14X WT expression). In comparison, the abundance of putative HSP30 decay fragments remains high when catalytically inactive Rny1 is expressed in *rny1Δ* strains (1.19X WT expression). The magnitude of these changes was relatively small however, meaning that while no definitive conclusions can be made, the hypothesized involvement of Rny1 activity in *HSP30* decay fragment clearance during the post-diauxic phase remains plausible.

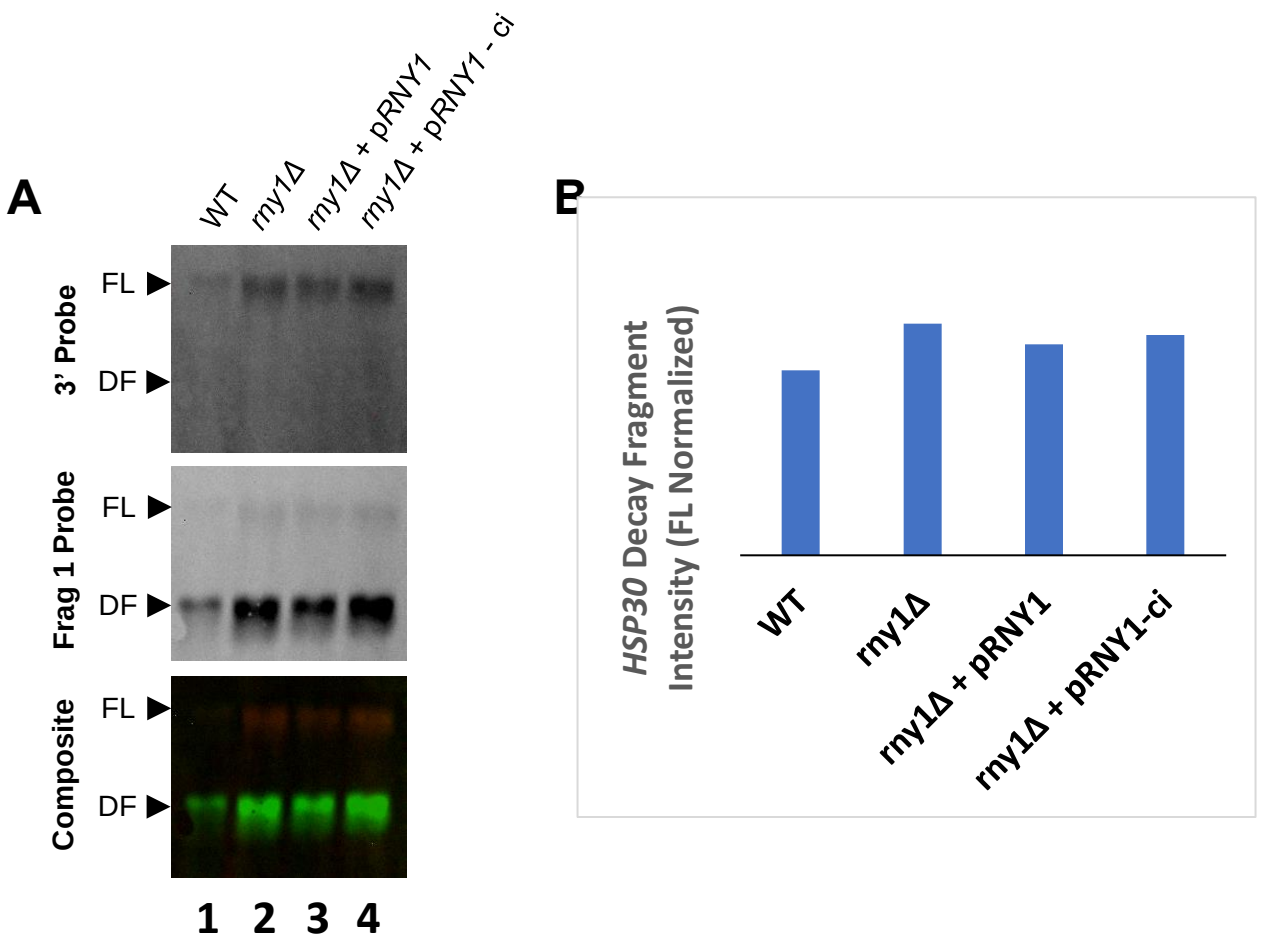

Figure 8: Rny1 activity is involved in the clearance of endogenous *HSP30* fragments. (A) Full length *HSP30* (highlighted with a black arrow and labeled DF) is detected using the IR700 probe that hybridizes to the 3' end of the transcript. The relative abundance of the WT full length *HSP30* appears to be lower, while the intensity is relatively similar across the other three strains. Both full length *HSP30* and the 5' fragment (highlighted with a black arrow and labeled DF) are detected by the IR800 probe that hybridizes within the putative sequence of fragment 1. We see a greater relative intensity of the fragment signal in the *rny1Δ* and *rny1Δ* + p*RNY1*–ci strains, suggesting that catalytically active Rny1 is involved in the clearance of these decay fragments. A relative decrease in decay fragment intensity is observed when catalytically active Rny1 is added to the *rny1Δ* strain, again suggesting Rny1 involvement in decay fragment clearance. The composite image shows both probes hybridizing to putative full length *HSP30* while only the frag 1 probe binds the 5' fragment as predicted. (B) The relative intensity of the *HSP30* decay fragment bands relative to the intensity of full-length *HSP30*.

Rny1 involvement in HSP30 decay fragment clearance is supported by RNase H digest.

In order to verify the assigned identifications of full-length RNA and decay fragments associated with *HSP30*, an RNase H digest targeted towards these two species was performed. In both RNase H-treated and -untreated samples, detection of full-length *HSP30* using the 3' probe appears to have been highly impaired, as shown by the lack of a prominent red signal

across all lanes. In comparison, detection of putative *HSP30* decay fragments using the frag 1 probe is robust in lanes 1, 4, and 7-9, as shown by the defined green bands appearing below very faint full-length bands in these lanes (Figure 9). RNase H treatment targeting either full-length *HSP30* or fragment 1 alone seems to prevent production of decay fragments (Lanes 2,3, 5, and 6, Figure 9). This may be due to *in vitro* decay after RNase H cleavage or an inability to detect the resulting cleaved RNA molecules. Because RNase H was targeted to *HSP30* transcripts using a specific oligonucleotide probe, this supports the identification of these bands as *HSP30*-related. However, the results are far from expected. RNase treatment targeted towards the full-length *HSP30* transcript was expected to cause a shift in the location of the full-length band without impairing fragment 1 formation (Lanes 2 and 5, Figure 9). Instead, we see highly impaired fragment 1 formation, potentially due to off-target cutting, inability to detect the smaller shifted bands, or incorrect identification of the HSP30 fragment band. RNase H targeted towards fragment one of the *HSP30* transcript was expected to cause a shift in the location of the full-length band and the fragment 1 band (Lanes 3 and 6, Figure 9). Instead, we see highly impaired fragment 1 formation off-target cutting or the incorrect identification of the HSP30 band as previously stated. A repeated trial with RNase H treatment without a targeting probe must be completed to rule out the potential for off-target cutting.

Looking beyond the RNase H treated lanes, a visual analysis suggests that the abundance of *HSP30* decay fragments is higher in the *rny1Δ* strain (Lane 4, Figure 9) relative to the WT strain (Lane 1, Figure 9). This relative overabundance is maintained in the *rny1Δ* strain expressing catalytically inactive Rny1 (Lane 8, Figure 9) but is not visually apparent in the *rny1Δ* strain expressing catalytically active Rny1 from a plasmid. These trends in the abundance of *HSP30* decay fragments are supported by the full-length *HSP30* normalized data. Looking at the non-RNase H treated samples only, we see a relative increase in the amount of putative *HSP30* decay fragments that are present when Rny1 is knocked out. This relative increase is largely reversed by the expression of catalytically active Rny1 from a plasmid but is only minorly

decreased by the expression of catalytically inactive Rny1. This data strongly supports that Rny1 is involved in the clearance of *HSP30* decay fragments. However, the presence of an obvious signal in the *hsp30Δ* strain is cause for concern (Lane 9, Figure 9). Because no *HSP30* mRNA should be expressed in this strain, the presence of any signal suggests that off-target binding may be occurring, potentially confounding the results from other lanes or negating the findings from HSP30 detection.

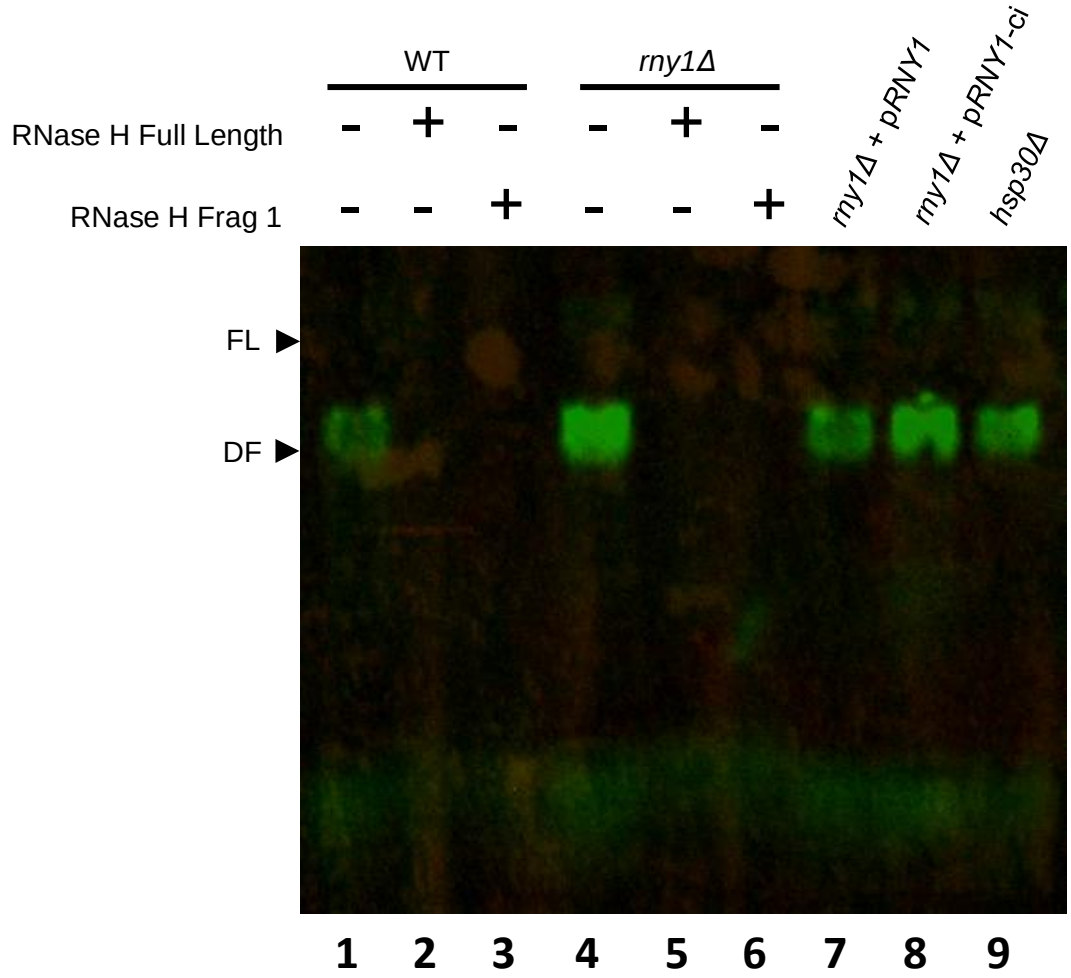

Figure 9: Mixed results from *HSP30* endogenous decay fragment verification. Very faint full length *HSP30* (highlighted with a black arrow and labeled FL) is visible in lanes 1, 4, 7, 8, and 9. Putative *HSP30* decay fragment 1 (highlighted with a black arrow and labeled DF) is visible in the same lanes. The relative intensity of the putative decay fragment band is highest in the *rny1Δ* and *rny1Δ* + p*RNY1*-ci strains, suggesting that catalytically active Rny1 is required for decay fragment clearance. The intensity of the decay fragment band is lower in the WT and *rny1Δ* + p*RNY1* strains. There is a nonzero signal in the *hsp30Δ* strain which was not expected. The RNase H treated samples should have shown shifted signals rather than the absence of signals, however, no signals are observed. This suggests that RNase H treatment caused the degradation of the resulting products or the signal is not intense enough for detection.

Discussion.

In order to better understand RNA dynamics in eukaryotes, we investigated how persistent RNA decay fragments are cleared in *S. cerevisiae*. Specifically, we investigated the involvement of the sole vacuolar ribonuclease, Rny1, in the clearance of decay fragments produced from the MS2 array and the endogenous *HSP30* transcript, whose existence was previously demonstrated by Garcia *et al*. Using an optimized northern blot procedure, we investigated steady state levels of full-length *PGK1-24xMS2* and endogenous *HSP30* transcripts and the relative abundance of the putative RNA decay fragments that they produce. By examining how the normalized amount of decay fragments differs based on the presence of Rny1 catalytic activity, we were able to infer an involvement of Rny1 endoribonuclease activity in the clearance of the examined RNA decay fragments.

With the chemiluminescent northern blot protocol we developed, we were first able to provide strong support for the Xrn1-dependent formation of MS2 decay fragments from the *PGK1-24xMS2* construct. The hypothesized route of MS2 decay fragment formation involves the 5' to 3' degradation by cytoplasmic RNA decay enzymes such as Xrn1.**Error! Bookmark not defined.** Understanding this process, and its relation to normal RNA decay mechanics, is essential for understanding the temporal and mechanistic aspects behind the different routes of post-transcriptional regulation. While this pathway was the predicted mechanism behind the formation of MS2 decay fragments, analyzing their steady-state levels in an *xrn1Δ* strain provided the most conclusive evidence that this cytoplasmic exoribonuclease was one of the primary agents responsible for their creation. It appears that *Xrn1*-deficient strains show greatly impaired formation of MS2 decay fragments when normalizing to full-length *PGK-24xMS2*. There is a robust accumulation of full-length *PGK1-24xMS2*, suggesting impaired degradation of this transcript, and a decreased abundance of MS2 decay fragments when normalizing to the precursor *PGK1-24xMS2*. Because MS2 decay fragment formation and full-length *PGK1-24xMS2* degradation are impaired by *Xrn1* knockout, this enzyme's involvement in incomplete

degradation and the resultant production of RNA decay fragments is highly supported. Because Xrn1 activity in *S. cerevisiae* seems to be intimately tied to RNP granules, the demonstrated connection between Xrn1 and RNA decay fragment formation supports the predicted pathway of decay fragment transport to the vacuole through the autophagic targeting of RNP granules. The shift of Xrn1 to eisosomes and a transition to decreased degradative activity in the post-diauxic phase in *S. cerevisiae* points to an increased important of alternative routes of decay during these changes,[ix] with a potentially upregulated reliance on the autophagy-mediated route of RNA decay that is currently hypothesized.

The predicted formation of endogenous decay fragments from the *HSP30* transcript was also supported during northern blot. Although the decay machinery involved in incomplete cytoplasmic degradation has not yet been identified, the appearance of a clear full-length and decay fragment band identified with the appropriate probes suggests that this process is occurring. To verify that the putative *HSP30* full-length and decay fragment species were correctly identified, targeted RNase H digest of these species was performed. RNase targeting both the full-length and decay fragment portions of the transcript resulted in no decay fragment band being observed. This could be due to residual RNA decay of the destabilized fragments *in vitro*, an inability to detect the shifted bands, or off-target RNase H activity. To eliminate the possibility that RNase H performed off targeting cutting that degraded all RNA species, the procedure will be repeated with RNase H applied without a targeting probe. The blot will also be run with higher stringency hybridization and wash conditions, to eliminate the possibility of off-target binding, which is suggested by the presence of a signal in the *hsp30*Δ strain. To further support the identification of HSP30-related species, *HSP30* knockout will be verified in the available strains using PCR, thus ensuring that no endogenous *HSP30* transcripts are being produced.

Having supported the predicted formation of persistent RNA decay fragments through the action of cytoplasmic decay enzymes, we could investigate the alternative routes of

degradation responsible for the clearance of these persistent molecules. Because of the connection between decay fragment formation, RNP granules, and the involvement of autophagy in RNP granule clearance, a potential autophagy-mediated route of degradation was hypothesized.[Error! Bookmark not defined.,Error! Bookmark not defined.,Error! Bookmark not defined.,Error! Bookmark not defined.] To begin demonstrating support for this putative pathway, we first sought to demonstrate that the sole vacuolar ribonuclease, Rny1, is involved in the clearance of decay fragments. If this hypothesis was supported, then autophagic targeting of decay fragments to the vacuole in yeast would be a highly plausible mechanism. We observed that the absence of Rny1 catalytic activity was associated with higher steady-state levels of MS2 decay fragments when normalizing to the amount of full-length *PGK1-24xMS2* present. *rny1Δ* strains or strains expressing only catalytically-inactive Rny1 from a plasmid showed an accumulation of decay fragments relative to WT yeast and yeast expressing only catalytically-active Rny1 from a plasmid, which often showed similar steady-state levels of decay fragments. The apparent evidence that the catalytic activity of a vacuolar ribonuclease is required for the normal clearance of MS2 decay fragments suggests either an intimate association between decay fragments and the vacuole, likely mediated through the process of autophagy, changing localization patterns for Rny1, or secondary effects of *Rny1* knockout. Microscopy studies investigating the localization of Rny1 and MS2-containing RNA could provide additional evidence supporting the direct degradative activity of Rny1 on MS2 decay fragments.

Despite the highly suggestive results from the original blots, several areas of confusion and avenues for improvement remain. In addition to improving blot sensitivity, reducing background signal, and utilizing higher-quality RNA, exploration of apparent discrepancies between normalization to the *7S* RNA control and full-length *PGK1-24xMS2* would aid in analysis of MS2 decay fragment clearance. Consistently, the observed MS2 decay fragment signal matched the predicted pattern of intensity when normalizing to full-length *PGK1-24xMS2*, but deviated from expected when normalizing to the constitutively expressed *7S* RNA control.

Rather than a systematic error in the northern blot procedure, it is likely that differences between strains cause differences in either *7S* or *PGK1-24xMS2* expression that confound apparent differences in MS2 decay fragment abundance. One notable trend that was observed is that the intensity of the full-length *PGK1-24xMS2* band in *rny1 Δ* strains is consistently greater than that of WT strains even when this increase is not reflected by the *7S* RNA control. This suggests that *Rny1* knockout may be upregulating *PGK1-24xMS2* expression in the post-diauxic relative to WT in a way that is not reflected by global changes in RNA expression. Recent evidence from the Garcia laboratory suggests that *Rny1* knockout is associated with an accelerated rate of glucose consumption. Because of this, *rny1Δ* strains may exhaust the available glucose more rapidly, causing them to enter the post-diauxic phase earlier compared to WT cells. Because all strains were grown over the same time period, this means that *rny1Δ* strains may have been deeper into the post-diauxic phase at the time of sampling. *PGK1-24xMS2* is expressed from the *Adh1* promoter that normally controls the gene encoding alcohol dehydrogenase 1, an enzyme that is intimately involved in ethanol usage during the post-diauxic phase. If *rny1Δ* yeast are deeper into post-diauxic at the time of sampling, then the expression of post-diauxic relevant genes such as *adh1* may be upregulated, causing greater expression from the *Adh1* promoter, leading to increased *PGK1-24xMS2* production. In order to account for this potential discrepancy, studies examining when *rny1Δ* and WT cells enter the post-diauxic are necessary. Altering the out-growth period for each strain could be used to perform RNA isolation at a standardized point in the yeast growth cycle, creating more consistent expression of full-length *PGK1-24xMS2* and the MS2 decay fragments produced from them. This may eliminate some of the observed discrepancies between *7S* and full-length *PGK1-24xMS2* expression, creating more reliable analyses of relative MS2 decay fragment abundance between strains.

Analysis of Rny1-dependent clearance of *HSP30* decay fragments yielded similar results with several unexpected signals that demand additional investigation. Initial analysis

demonstrated the clear presence of two distinct bands. The patterns of probe binding suggested that the upper band consisted of the full-length *HSP30* transcript while the lower band was the upstream fragment produced from incomplete cytoplasmic degradation. Because the two putative *HSP30* signals seemed to appear in the same location on the membrane as the prominent *25S* rRNA and *18S* rRNA bands, there was initial concern over off-target binding of the *HSP30* probes to abundant RNA species. However, the patterns of probe binding suggested that this may not be the case. Normalizing to the intensity of the putative full-length *HSP30* transcript, a slight abundance of fragment 1 was observed in the absence of Rny1 activity relative to WT, in the *rny1Δ* strain and the *rny1Δ* strain with catalytically-inactive Rny1 expressed from a plasmid. A minor relief of this apparent abundance was observed when catalytically active Rny1 was expressed from a plasmid in an *rny1Δ* strain. Overall, this pattern of normalized fragment intensity does suggest an involvement of Rny1 in the clearance of endogenous decay fragments from *HSP30*. Similar to the MS2 findings, the observation that the sole vacuolar ribonuclease may be involved in the clearance of endogenous decay fragments suggests that an alternative route of decay involving the targeting of decay fragments to the vacuole may be important for specific RNA species or during specific stages of yeast growth. This interaction is likely mediated by autophagy and may involve RNP granules, where much of the RNA decay machinery and likely the products of incomplete cytoplasmic degradation localize. Having observed this process for endogenous transcripts, we can hypothesize that Rny1 may be involved in the clearance of clearance of certain RNA species, with possible particular importance in the degradation of persistent RNA molecules. The observation of this for an endogenous transcript without an engineered and highly stable secondary structure highlights a broader importance of this potential alternative clearance route. The investigation of additional transcripts identified as producing endogenous decay fragments could support this hypothesis.

An understanding of Rny1's involvement in the clearance of engineered and endogenous decay fragments has broad implications for our understanding of post-transcriptional regulation and human pathology. Understanding the differences in primary routes of RNA decay based on cellular environment and RNA target is integral in understanding RNA dynamics and post-transcriptional regulation as a whole. For example, in *S. cerevisiae*, the cytoplasmic decay enzyme Xrn1 undergoes changes in localization and activity in response to changing nutrient conditions,[ix] potentially placing increased weight on alternative decay routes. This includes the potential autophagy-mediated route of vacuolar decay supported by our results. Understanding the types of RNA molecules that are degraded by these alternative pathways and the conditions under which these pathways are upregulated is extremely important in understanding how certain classes of RNA are post-transcriptionally regulated.

Autophagy is a highly conserved process in eukaryotes for the transport of material to the vacuole or the lysosome.[xi] Our research suggests that the T2 family RNase Rny1 in yeast is involved in the clearance of persistent decay fragments in the post-diauxic phase. As the sole vacuolar ribonuclease, it is hypothesized that autophagy, potentially targeting RNP granules, is involved in connecting incomplete cytoplasmic decay of some transcripts to their ultimate vacuolar clearance by Rny1. This process is of surprising relevance in cases of pathological neurodegeneration of higher eukaryotes, including humans. Genetic markers of neurogenerative diseases such as ALS have already been associated with autophagy, RNA binding proteins, and other agents affecting RNP granule dynamics.**Error! Bookmark not defined.** Recently, a more direct connection between lysosomal/vacuolar T2 RNases and neurological conditions has been discovered in zebrafish models.[vii] In this model organism, inactivity of the lysosomal ribonuclease rnaset2 appears to cause an associated increase in white matter lesions, regions of abnormal myelination in the brain. This connection between rnaset2 and white matter lesions is hypothesized to be due to the lysosomal engorgement and impairment by accumulating rRNA and altered dynamics with amyloid precursor proteins in the sites of

neurodegeneration. RNase T2 mutations in humans have already been associated with the neurological condition leukoencephalopathy. Our research demonstrates a distant connection between the role of the sole vacuolar ribonuclease from the T2 family in *S. cerevisiae*, the clearance of persistent RNA species under conditions of nutrient-related stress in yeast, and neurodegeneration in higher eukaryotes through impaired lysosomal function and the accumulation of amyloid plaques. The impaired activity of T2 family RNases involved in the degradation of autophagy-targeted RNAs may serve as a unifying factor explaining the accumulation of RNA decay fragments in *S. cerevisiae* and some neurodegenerative processes in higher eukaryotes.

Acknowledgements.

I would like to thank the endless support and kindness from my advisor and research mentor, Dr. Jennifer Garcia. Her assistance in technical and experimental design matters has been invaluable in my journey as a developing independent scientist. I would also like to thank my lab partners, Megan K. and Sally M. The productive and fun environment they helped develop in the lab was fully appreciated. Finally, I would like to thank the NSEC Research and Development Grant and the Boettcher Foundation for their generous funding.

Tables.

Table 1: Probe Sequences for Northern Blot

Probe	Sequence
7S Probe	5'-GTCTAGCCGCGAGGAAGG-3'
Oligo(dT) Probe	5'-TTTTTTTTTTTTTTTTTTTTTTTTTT-3'
3' MS2 Probe #1	5'-CTAGAACTAGTACTCACTATAGGGCGAATTG-3'
5' MS2 Probe	5'-AATAAGTACCGTAGGATCCAAGGG-3'
Internal MS2 Probe	5'-CTCGTGCTTTCTTGGCAATAAGTA-3'
3' MS2 Probe #2	5'-CCTTAGATCTGATGAACCCTGGAAT-3'

Literature Cited.

[i] Balagopal, V., Fluch, L., & Nissan, T. (2012). Ways and means of eukaryotic mrna decay. *Biochimica Et Biophysica Acta (BBA) - Gene Regulatory Mechanisms*, *1819*(6), 593–603. https://doi.org/10.1016/j.bbagrm.2012.01.001

[ii] Garcia, J. F., & Parker, R. (2015). MS2 coat proteins bound to yeast mrnas block 5′ to 3′ degradation and trap mrna decay products: Implications for the localization of mrnas by MS2-MCP system. *RNA*, *21*(8), 1393–1395. https://doi.org/10.1261/rna.051797.115

[iii] Huang, H., Kawamata, T., Horie, T., Tsugawa, H., Nakayama, Y., Ohsumi, Y., & Fukusaki, E. (2014). Bulk RNA degradation by nitrogen starvation-induced autophagy in yeast. *The EMBO Journal*, *34*(2), 154–168. https://doi.org/10.15252/embj.201489083

[iv] Makino, S., Kawamata, T., Iwasaki, S., & Ohsumi, Y. (2021). Selectivity of mrna degradation by autophagy in yeast. *Nature Communications*, *12*(1). https://doi.org/10.1038/s41467-021-22574-6

[v] Reggiori, F., & Klionsky, D. J. (2013). Autophagic processes in yeast: Mechanism, machinery and regulation. *Genetics*, *194*(2), 341–361. https://doi.org/10.1534/genetics.112.149013

[vi] MacIntosh, G. C., Bariola, P. A., Newbigin, E., & Green, P. J. (2001). Characterization of RNY1, the saccharomyces cerevisiae member of the T2 RNase family of RNases: Unexpected functions for ancient enzymes? *Proceedings of the National Academy of Sciences*, *98*(3), 1018–1023. https://doi.org/10.1073/pnas.98.3.1018

[vii] Haud, N., Kara, F., Diekmann, S., Henneke, M., Willer, J. R., Hillwig, M. S., Gregg, R. G., MacIntosh, G. C., Gärtner, J., Alia, A., & Hurlstone, A. F. (2011). rnaset2 mutant zebrafish model familial cystic leukoencephalopathy and reveal a role for RNase T2 in degrading ribosomal RNA. *Proceedings of the National Academy of Sciences*, *108*(3), 1099–1103. https://doi.org/10.1073/pnas.1009811107

[viii] Jones, C. I., Zabolotskaya, M. V., & Newbury, S. F. (2012). The 5′ → 3′ exoribonuclease xrn1/pacman and its functions in cellular processes and development. *Wiley Interdisciplinary Reviews: RNA*, *3*(4), 455–468. https://doi.org/10.1002/wrna.1109

[ix] Grousl, T., Opekarová, M., Stradalova, V., Hasek, J., & Malinsky, J. (2015). Evolutionarily conserved 5'-3' exoribonuclease XRN1 accumulates at plasma membrane-associated eisosomes in post-diauxic yeast. *PLOS ONE*, *10*(3). https://doi.org/10.1371/journal.pone.0122770

[x] Piper, P. W., Ortiz-Calderon, C., Holyoak, C., Coote, P., & Cole, M. (1997). HSP30, the integral plasma membrane heat shock protein of saccharmyces cerevisiae, is a stress-inducible regulator of plasma membrane h+-atpase. *Cell Stress & Chaperones*, *2*(1), 12. https://doi.org/10.1379/1466-1268(1997)002<0012:htipmh>2.3.co;2

[xi] Ohsumi, Y. (2013). Historical landmarks of Autophagy Research. *Cell Research*, *24*(1), 9–23. https://doi.org/10.1038/cr.2013.169